Int. Journal of Refractory Metals & Hard Materials 28 (2010) 383–387

Contents lists available at ScienceDirect

Int. Journal of Refractory Metals & Hard Materials

journal homepage: www.elsevier.com/locate/IJRMHM

An investigation about the activation energies of the reduction transitions of fine dispersed $CuWO_{4-x}/WO_{3-x}$ oxide powders

M. Ardestani [a,*], H. Arabi [a], H. Razavizadeh [a], H.R. Rezaie [a], B. Jankovic [b], S. Mentus [b]

[a] Department of Materials and Metallurgical Engineering, Iran University of Science and Technology, Narmak, Tehran 16846-13114, Iran
[b] Faculty of Physical Chemistry, University of Belgrade, Studentski Trg 12-16, P.O. Box 137, 11001 Belgrade, Serbia

ARTICLE INFO

Article history:
Received 29 July 2009
Accepted 11 December 2009

Keywords:
W–Cu oxides
Activation energy
Reduction

ABSTRACT

Non-isothermal reduction of fine dispersed $CuWO_{4-x}/WO_{3-x}$ oxide phases were investigated by thermogravimetry (TG) and differential thermogravimetry (DTG) analyses under hydrogen atmosphere and the activation energies of the corresponding reduction transitions determined by Kissinger–Akaira–Sunose (KAS) and Flynn–Wall–Ozawa (FWO) methods. The activation energy of the first reduction stage ($CuWO_{4-x} \xrightarrow{I} Cu + WO_{3-x}$) using the mentioned methods were defined as $E_{KAS(stepI)} = 34\ kJ\ mol^{-1}$ and $E_{FWO(stepI)} = 41\ kJ\ mol^{-1}$, respectively. Also, the "*E*" values were determined as $E_{KAS(stepII)} = 91.8\ kJ\ mol^{-1}$ and $E_{FWO(stepII)} = 101\ kJ\ mol^{-1}$ for the second and $E_{KAS(stepIII)} = 147.2\ kJ\ mol^{-1}$ and $E_{FWO(stepIII)} = 156.3\ kJ\ mol^{-1}$ for the third reduction steps ($WO_{3-x} \xrightarrow{II} WO_2 \xrightarrow{III} W$), respectively. The results showed that copper from one side helps ($WO_2 \rightarrow W$) reduction to start at lowered temperatures, but, from the other side, it enlarges the activation energy of this reaction by about 20 kJ mol^{-1}. This increase explained by the fact that copper acts as a barrier for formation and transportation of volatile $WO_2(OH)_2$ compound which is the main agent responsible for reduction of tungsten oxide.

1. Introduction

Recently, a new process was applied to synthesis W–Cu composite powders with nanoscale dispersion of the constituents (i.e. tungsten and copper) and high sinterability at relatively low sintering temperatures. The process included initial precipitation of W–Cu compounds from the solution containing the corresponding W and Cu ions, calcination the precipitates and reduction the calcined compounds [1,2]. Based on the previous investigations [1,2], calcination of the initial precipitates is due to evaporation of the volatile constituents such as H_2O and NH_3 and formation of $CuWO_{4-x}$ and WO_{3-x} oxide phases. As expressed previously, these oxides could be reduced under hydrogen atmosphere to W–Cu composite powders. In general, Cu oxide phases, such as CuO may be reduced by hydrogen at relatively low temperatures [3]. However, reduction of tungsten oxides and particularly WO_3 requires high temperatures and is more complicated due to formation of intermediate phases during the reduction period [4–6]: $WO_3 \rightarrow WO_{3-x} \rightarrow WO_2 \rightarrow W$. On the basis of morphological investigations [6], reduction of tungsten oxides can be postulated by oxygen and tungsten transport mechanisms. In the case of oxygen transport mechanism, the direct oxygen removal from the solid oxides is responsible for the reduction process. However, this mechanism is characterized for low reduction temperatures (below 1023 K) and particularly for reduction of WO_3 to $WO_{2.9}$. The second mechanism which is the main suggested process for reduction of tungsten oxides is based on chemical vapor transport of tungsten by the volatile $WO_2(OH)_2$ [6–8]. Although the reduction mechanism of tungsten oxides has been investigated in detail, the kinetics aspects such as activation energies of reduction stages of this process especially in presence of copper have not been properly clarified. Therefore, in this study, the non-isothermal reduction of fine dispersed $CuWO_{4-x}$ and WO_{3-x} oxide phases, synthesized by the above mentioned method, have been investigated using TG and DTG analyses. The activation energy of each detected reduction stage was determined using both KAS and FWO methods. Furthermore, the effect of Cu on $WO_2 \rightarrow W$ transition is discussed.

2. Experimental

Fine dispersed $CuWO_{4-x}/WO_{3-x}$ oxide powders were synthesized by a precipitation method which has been described elsewhere [1,2]. The pure WO_3 oxide powder was synthesized by calcination of ammonium para tungstate (APT) at 873 K in air atmosphere for 1.5 h. Thermogravimetric analysis of the oxide samples was carried out in a TA SDT 2960 device under reducing gas stream (25 vol.% H_2 + Ar, 99999% purity), at heating rates of 2.5, 5 and 15 K min^{-1}, in a temperature interval from 300 to

* Corresponding author. Tel.: +98 22413892; fax: +98 2177240480.
E-mail address: mohammadard@yahoo.com (M. Ardestani).

0263-4368/$ - see front matter © 2009 Elsevier Ltd. All rights reserved.
doi:10.1016/j.ijrmhm.2009.12.003

1223 K. In order to confirm the repeatability and authenticity of the generated data for all cases the experiments were repeated three times at every heating rate and the average TG trace among them was used as the representative thermo-analytical curve in the present manuscript. The observed deviations were very little.

The microstructures of the oxide compounds and the reduced powders were evaluated using Scanning Electron Microscopy (SEM-PHILIPS-XL30).

3. Theoretical backgrounds for calculation of activation energy

In order to determine the rate of the reaction for non-isothermal experimental condition, the following equation could be used [9–11]:

$$\frac{d\alpha}{dt} = K(T)f(\alpha) = A\exp\left(-\frac{E_a}{RT}\right)f(\alpha) \quad (1)$$

where $K(T)$ is the rate constant, A the pre-exponential factor, E_a the apparent activation energy, R the universal gas constant, T the absolute temperature and $f(\alpha)$ is the reaction model (α parameter is the conversion fraction at any temperature: $\alpha = (m_0 - m_T)/(m_0 - m_f)$ where m_0, m_T and m_f are the beginning, actual and final mass of the sample, respectively).

For a sample with a constant heating rate (i.e. $\beta = \frac{dT}{dt} = cte.$) it can be written:

$$\beta\frac{d\alpha}{dT} = A\exp\left(-\frac{E_a}{RT}\right)f(\alpha) \quad (2)$$

Integrating Eq. (1) gives the integral form of non-isothermal rate law:

$$g(\alpha) = \frac{A}{\beta}\int_0^T \exp\left(-\frac{E_a}{RT}\right)dT \quad (3)$$

in which $g(\alpha)$ is the integral function of conversion and has no analytical solution. However, in order to write the above integral in a more general form, $\frac{E_a}{RT}$ is considered as x and if:

$$p(x) = \int_x^\infty \frac{\exp(-x)}{x^2}dx \quad (4)$$

Then Eq. (3) can be expressed as:

$$g(\alpha) = \frac{AE_a}{\beta R}p(x) \quad (5)$$

$p(x)$ can be approximated using two different methods:

(a) Flynn–Wall–Ozawa (FWO) method in which on the basis of Doyle approximation p(x) is assumed as:

$$\ln p(x) \approx -5.331 - 1.052x \quad (6)$$

Taking logarithm in Eq. (5) and replacing in Eq. (6) it can be written:

$$\ln\beta = \ln\left[\frac{AE_a}{Rg(\alpha)}\right] - 5.331 - 1.052\frac{E_a}{RT} \quad (7)$$

For a definite α, the plot of $\ln\beta$ vs. $\frac{1}{T}$ for different heating rates should be a straight line which the activation energy can be calculated by multiplying the slope of this line by $\frac{R}{1.052}$.

(b) Kissinger–Akaira–Sunose (KAS) method in which $p(x)$ is assumed as:

$$p(x) = \frac{\exp(-x)}{x^2} \quad (8)$$

By substituting Eq. (8) into Eq. (5) and taking logarithm the following equation can be obtained:

$$\ln\left(\frac{\beta}{T^2}\right) \cong \ln\left[\frac{AR}{g(\alpha)E_a}\right] - \frac{E_a}{RT} \quad (9)$$

Multiplying the slope of the line which is the plot of $\ln\left(\frac{\beta}{T^2}\right)$ vs. $\frac{1}{T}$ by R, gives the apparent activation energy of the reaction.

4. Results and discussion

4.1. Determination of the activation energies of the reduction steps

Fig. 1 shows the SEM micrograph of $CuWO_{4-x}/WO_{3-x}$ oxide powders. This figure shows that the oxide particles have submicron size and polygonal shape.

Fig. 2a and b shows the TG and the corresponding DTG curves of the fine dispersed $CuWO_{4-x}/WO_{3-x}$ samples obtained at different heating rates. As it shown in this figure, three main weight loss stages can be detected in TG curves which are attributed to the following reaction steps [12,13]:

(1) $CuWO_{4-x} \rightarrow Cu + WO_{3-x}$

(2) $WO_{3-x} \rightarrow WO_2$

(3) $WO_2 \rightarrow W$

(It should be noted that in the mentioned reactions only the solid phases are considered).

The SEM image of the reduced powders is shown in Fig. 3. According to this figure the reduced powders have been agglomerated but it can be said that the size of each particle is lower than one micron.

The "T_{max}" of each reduction step is shown in Fig. 2b. According to the DTG curves it can be seen that the first DTG peaks (at all heating rates) are very narrow, but the third ones have shoulders (see heating rates of 2.5 and 5 K min^{-1}). Moreover, it is observed that by increasing the heating rate, a lateral shift of T_{max} is occurred for each reaction. This may due to the combined effects of the heat transfer at the different heating rates and the kinetics of reduction process resulting in delayed reduction [14].

As it is shown in Fig. 2, by increasing the heating rate, the weight loss steps and their corresponding DTG peaks were shifted to higher temperatures. Fig. 4 shows the experimental conversion ($\alpha - T$) curves for non-isothermal reduction of fine dispersed $CuWO_{4-x}/WO_{3-x}$ oxide phases for three reduction stages at different heating rates. It can be observed that by increasing the heating rates (β), the rate of the reduction process increases too.

Fig. 5 shows the determined apparent activation energy of the reduction steps which have been determined by FWO and KAS methods. As it can be observed, the values of the apparent activation energies for the reduction steps are same for different α values. This shows that all of the reduction steps may be formally treated as a single-step reaction [11]. According to this figure it

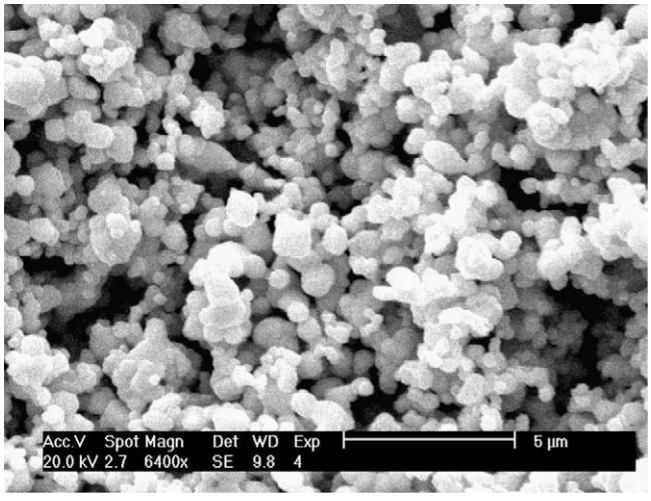

Fig. 1. SEM micrograph of $CuWO_{4-x}/WO_{3-x}$ oxide powders.

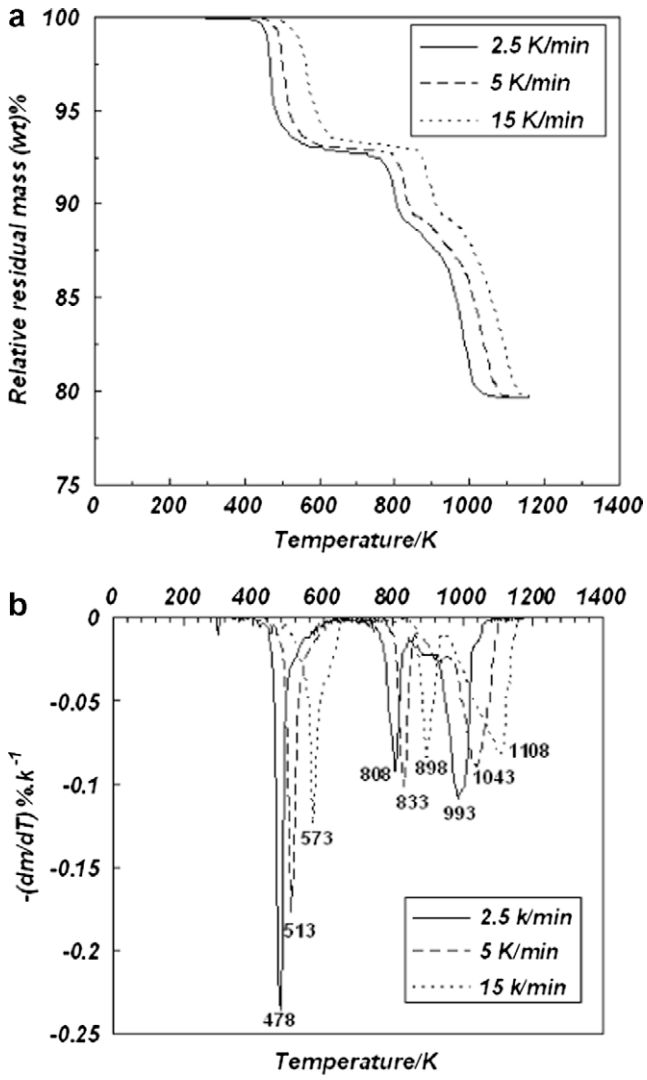

Fig. 2. (a) TG and (b) DTG curves for non-isothermal reduction of fine dispersed $CuWO_{4-x}/WO_{3-x}$ oxide phases in hydrogen atmosphere. T_{max} of DTG peaks are shown at different heating rates.

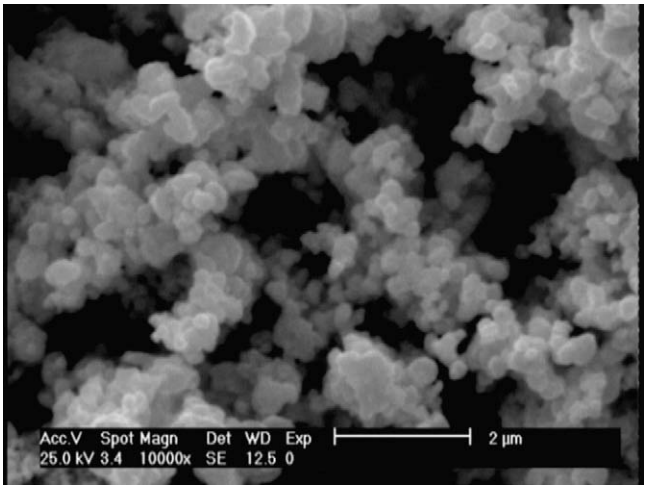

Fig. 3. SEM micrograph of the reduced powders.

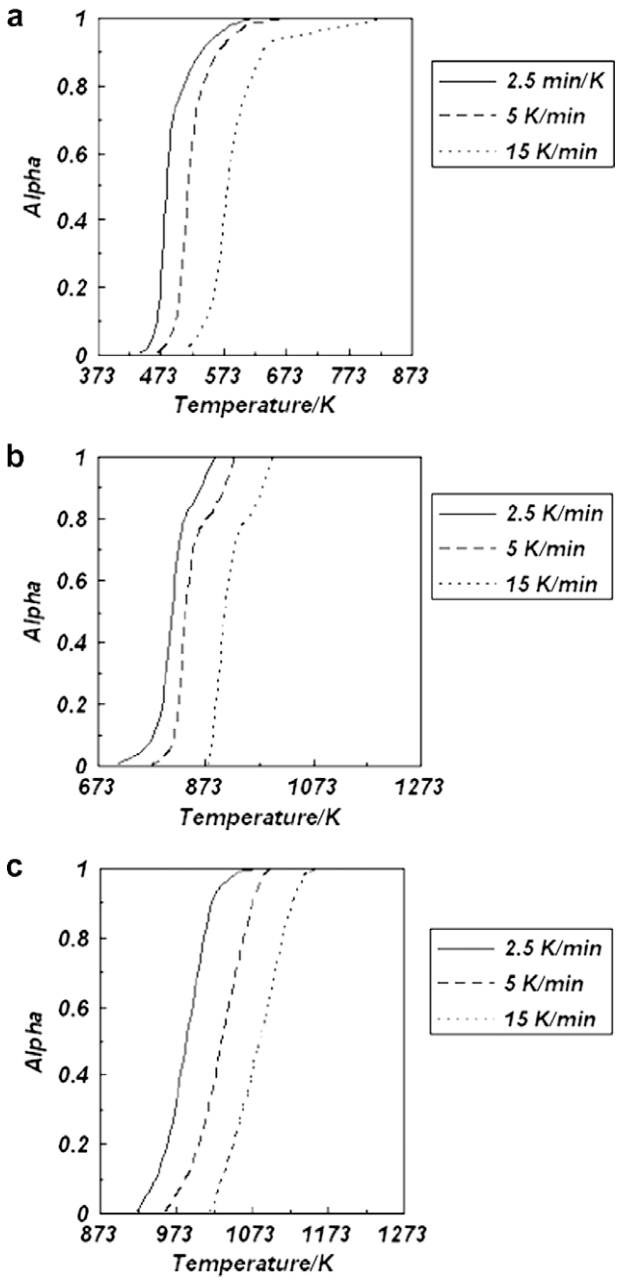

Fig. 4. The experimental conversion curves for (a) first (b) second and (c) third stage reduction of fine dispersed $CuWO_{4-x}/WO_{3-x}$ oxide phases in hydrogen atmosphere.

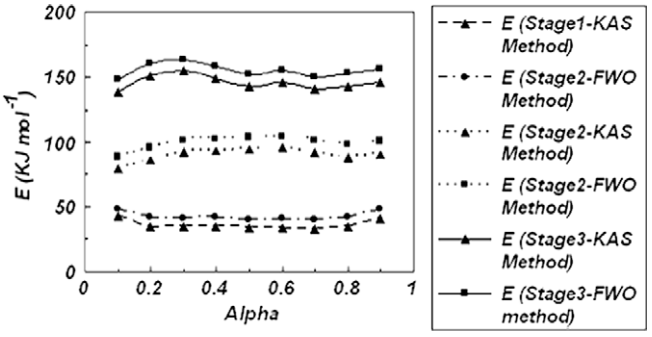

Fig. 5. Dependence of the apparent activation energies of reduction on the conversion degree.

Table 1
E_{AVE} values for the reduction steps, calculated by FWO and KAS methods.

E_{AVE}	Stage No.		
	Stage 1	Stage 2	Stage 3
$E_{AVE\text{-}KAS}$ (kJ mol^{-1})	34	91.8	147.2
$E_{AVE\text{-}FWO}$ (kJ mol^{-1})	40.1	101	156.3

can be observed that for all of the three reduction stages, the activation energies which were calculated using FWO method is slightly higher than the calculated E value by KAS method. This is due to different assumed $p(x)$ functions in these two methods. However, the calculated values by KAS method are more reliable than that of FWO. This is due to very crude approximation of the temperature integral $p(x)$ used in FWO method [11]. The average values of the activation energies (E_{AVE}) for the three reduction steps are presented in Table 1. Worthy to note that in order to calculate the E_{AVE} values for the reduction stages, the average of the activation energies within $0.2 \leqslant \alpha \leqslant 0.8$ have been considered. The reason of this matter is that, in contrast to reactions in liquid solutions, in solid state, the reactions usually include well-known mass and heat transfer at both the initial and the final stages, which causes temperature and partial pressure gradient. Due to these phenomena, a reaction gradient is formed from the outer to the inner surface of the sample which is unavoidable. So, the apparent activation energies which are calculated in these stages may differ from the real value of "E" and it seems that it is more reliable to calculate the E_{AVE} value considering the middle stages data of solid state reactions.

4.2. Effect of Cu on reduction of tungsten oxide

Fig. 6 shows the obtained TG and DTG curves of pure WO_3 with different heating rates. As it is observed in the figures, three weight loss stages could be detected in these curves which are defined as [5,6,8]:

(1) $WO_3 \rightarrow WO_{3-x}$
(2) $WO_{3-x} \rightarrow WO_2$
(3) $WO_2 \rightarrow W$

In order to investigate the effect of Cu on the reduction of tungsten oxide using the experimental results of this research, it seems that only the reduction of WO_2 to W must be considered. The reason of this conclusion is that only this reaction is exactly similar in both reduction procedures (i.e. reduction of pure WO_3 and $CuWO_{4-x}/WO_{3-x}$ oxide phases). In other words because WO_{3-x} phase may differ for the different reduction processes due to various quantities of x such as 0.1 and 0.28, so the effect of Cu on the other transitions could not be investigated properly.

According to Figs. 2 and 6, the presence of copper reduces the transition temperature of WO_2 to W from 1048, 1083 and 1168 K to 993, 1043 and 1108 K for 2.5, 5 and 15 K^{-1} heating rates, respectively. This result is in good agreement with the result of Kim et al. [5]. They concluded that in the case of W–Cu oxide phases, pre-reduced copper acts as a site for hydrogen reduction of WO_2 to W by hydrogen transport mechanism. Fig. 7 shows the activation energy of the reduction of WO_2 to W which has been determined using FWO and KAS methods. Also, the E_{AVE} values of this transition using the mentioned methods were determined as 136.4 and 125.8 kJ mol^{-1}, respectively.

According to the obtained results, it can be concluded that although presence of copper reduced the temperature of conversion of WO_2 to W, this agent increased the activation energy of this transition. The reason of this phenomenon seems to be related to the mechanism of tungsten oxide reduction. Based on this mechanism, volatile $WO_2(OH)_2$ is formed by a surface reaction of WO_2 with $H_2O(g)$ [6]:

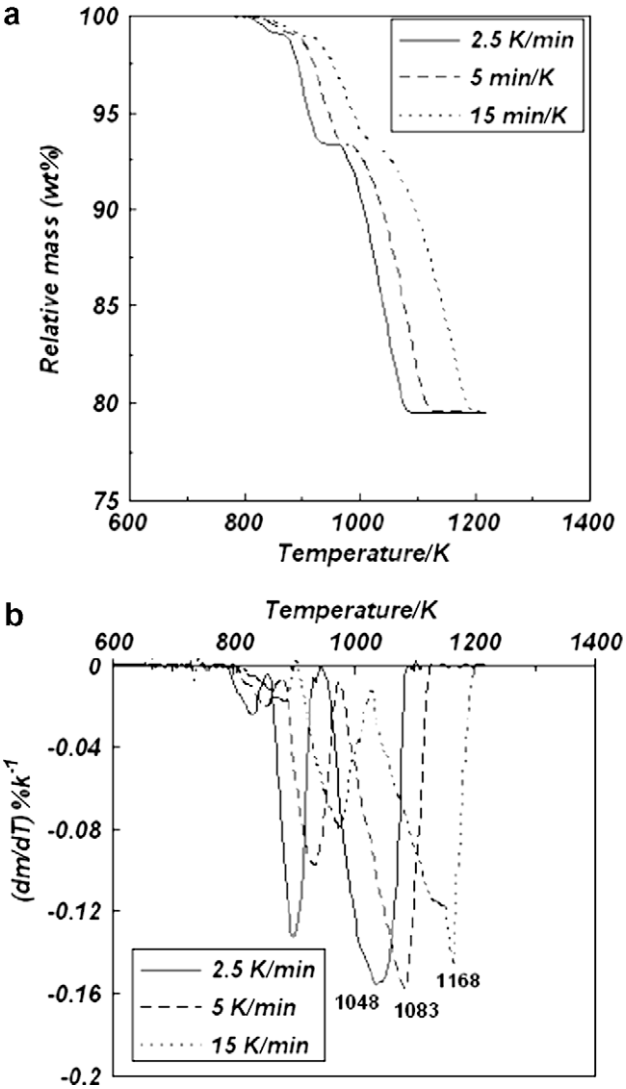

Fig. 6. (a) TG and (b) DTG curves for non-isothermal reduction of WO_3 by hydrogen.

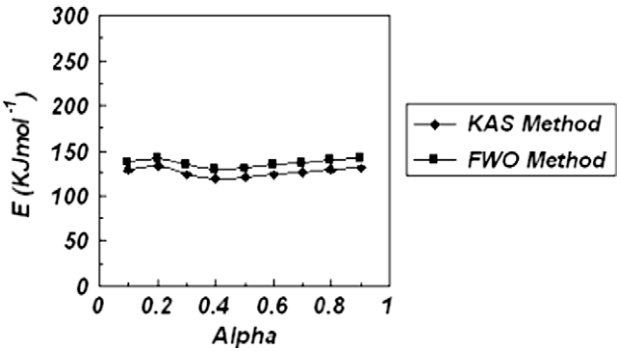

Fig. 7. Dependency of the apparent activation energy of WO_2 to W reduction on the conversion fraction.

$$WO_2(s) + 2H_2O(g) \rightarrow WO_2(OH)_2 + 2H_2$$

Then the volatile $WO_2(OH)_2$ is transported from WO_2 to W (Fig. 8). This chemical vapor transport is due to lower partial pressure of $WO_2(OH)_2$ above W respect to that of WO_2. Finally, the volatile compound reduces on the surface of W phase [6]. In presence

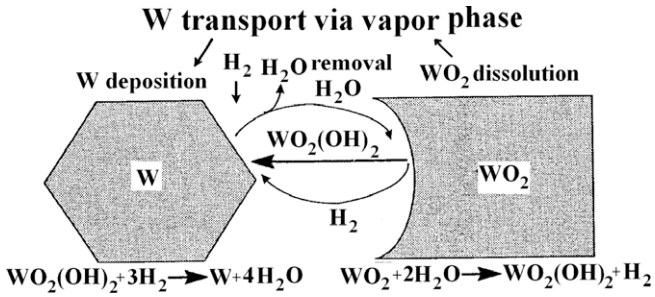

Fig. 8. Schematic presentation of WO_2 to W reduction by chemical vapor transport of tungsten [6].

of copper it seems that this agent acts as a barrier for transport of the volatile $WO_2(OH)_2$ which has been formed by the mentioned surface reaction between WO_2 and water vapor and as a result higher activation energy is needed to activate and resume the reduction process. Moreover, in the case of WO_2—Cu powders, the surface reaction between water vapor and WO_2 is reduced due to presence of pre-reduced copper and this may decrease the rate of the reduction.

5. Conclusion

(1) The activation energies of the reduction reactions of $CuWO_{4-x}/WO_{3-x}$ were determined using KAS and FWO methods. Using the mentioned methods, the following average values of the activation energies (E_{AVE}) were determined as:
   (a) $E_{KAS(stepI)} = 34\,kJ\,mol^{-1}$ and $E_{FWO(stepI)} = 41\,kJ\,mol^{-1}$ for $CuWO_{4-x} \rightarrow Cu + WO_{3-x}$.
   (b) $E_{KAS(stepII)} = 91.8\,kJ\,mol^{-1}$ and $E_{FWO(stepII)} = 101\,kJ\,mol^{-1}$ for $WO_{3-x} \rightarrow WO_2$.
   (c) $E_{KAS(stepIII)} = 147.2\,kJ\,mol^{-1}$ and $E_{FWO(stepIII)} = 156.3\,kJ\,mol^{-1}$ for $WO_2 \rightarrow W$.

(2) Copper decreases the reduction temperature of WO_2 to W reaction. However, this agent plays a barrier role for forming and transport of volatile $WO_2(OH)_2$ which is responsible for WO_2 reduction. This negative effect of copper is due to increasing the activation energy of $WO_2 \rightarrow W$ transition for about $20\,kJ\,mol^{-1}$.

References

[1] Ardestani M, Rezaie HR, Arabi H, Razavizadeh H. The effect of sintering temperature on densification of nanoscale dispersed W–20–40 wt% Cu composite powders. Int J Refract Met Hard Mater 2009;27:862–7.
[2] Ardestani M, Razavizadeh H, Arabi H, Rezaie HR. Preparation and sintering of W–20%wt Cu composite powders produced by co-precipitation method. Iranian J Mater Sci Eng 2009;6(2):24–9.
[3] Kim JY, Jose, Rodriguez A, Jonathan Hanson C, Frenkel AI, Lee PL. Reduction of CuO and Cu_2O with H_2: H embedding and kinetic effects in the formation of suboxides. J Am Chem Soc 2003;125:10684–92.
[4] Kim DG, Kyung HM, Chang SY, Oh ST, Lee CH, Kim YD. Effect of pre-reduced Cu on hydrogen reduction of W-oxide in WO_3–CuO powder mixtures. Mater Sci Eng 2005;399A:326–31.
[5] Kim GS, Lee YJ, Kim DG, Oh ST, Kim DS, Kim YD. The behavior of tungsten oxides in the presence of copper during hydrogen reduction. J Alloys Compd 2006;419:262–6.
[6] Lassner E, Schubert W. Tungsten. New York: Kluwer Academic Publishers/ Plenum Press; 1999.
[7] Hashempour M, Razavizadeh H, Rezaie HR, Salehi MT. Thermochemical preparation of W–25% Cu nanocomposite powder through a CVT mechanism. Mater Charact 2009;60:1232–40.
[8] Kim DG, Oh ST, J H, Lee CH, Kim YD. Hydrogen-reduction behavior and microstructural characteristics of WO_3–CuO powder mixtures with various milling time. J Alloys Compd 2003;354:239–42.
[9] Jankovic B. Kinetics analysis of the non-isothermal decomposition of potassium metabisulfite using the model-fitting and isoconventional (model-free) methods. Chem Eng J 2008;139:128–35.
[10] Jankovic B, Adnadjevic B, Mentus S. The kinetic study of temperature-programmed reduction of nickel oxide in hydrogen atmosphere. Chem Eng Sci 2008;63:567–75.
[11] Jankovic B, Mentus S, Jelic D. A kinetic study of non-isothermal decomposition process of anhydrous nickel nitrate under air atmosphere. Physica B 2009;404:2263–9.
[12] Yoon ES, Lee JS, Oh ST, Kim BK. Microstructure and sintering behavior of W–Cu nanocomposite powder produced by thermo-chemical process. Int J Refract Met Hard Mater 2002;20:201–6.
[13] Kim TH, Yu JH, Lee JS. The mechanism of hydrogen reduction synthesis of nanocomposite W–Cu. Nanostruct Mater 1997;9:213–6.
[14] Aboulkas A, Harfi KE, Bouadili AE. Pyrolysis of olive residue/low density polyethylene mixture: Part I Thermogravimetric kinetics. J Fuel Chem Tech 2008;36(6):672–8.